

# Solution-processed organic transistors based on semiconducting blends†

Jeremy Smith,<sup>a</sup> Richard Hamilton,<sup>b</sup> Iain McCulloch,<sup>b</sup> Natalie Stingelin-Stutzmann,<sup>c</sup> Martin Heeney,<sup>b</sup> Donal D. C. Bradley<sup>a</sup> and Thomas D. Anthopoulos<sup>\*a</sup>

Received 19th October 2009, Accepted 22nd January 2010

First published as an Advance Article on the web 16th February 2010

DOI: 10.1039/b921674j

The latest advances in the use of solution processable organic semiconductor blends for organic field effect transistor (OFET) applications are reviewed. We summarise multi-component, thin film microstructure formation from solution with particular focus on phase separation and crystallisation of components. These approaches can then be applied to semiconducting materials and their use in organic devices. Several key applications are studied, namely ambipolar systems with n- and p-type components, high charge carrier mobility and uniform films for high performance OFETs, and the potential for self-assembly during OFET fabrication. Blending materials can in all cases be used to combine the advantageous properties of the individual components.

## 1. Introduction and background

Organic semiconductor materials for electronics applications have advanced rapidly in the past few years resulting in higher charge carrier mobilities,<sup>1,2</sup> more easily processable films<sup>3</sup> and considerable progress in integrating these materials into useful

circuits.<sup>4</sup> One way to obtain the required properties for a particular device is to blend two or more organic components with the aim of combining the advantageous properties of each or even exceeding the performance of the individual components. Blending organics is easily achieved if the materials are soluble in a common solvent and can then be processed therefrom. Common examples of such devices include the bulk hetero-junction solar cell and blends for organic light emitting diodes, both of which have been extensively studied and reviewed.<sup>5,6</sup> This paper, however, will focus on their less well exploited but equally interesting use in thin-film organic field effect transistors (OFETs).

There are several important factors to consider when using a blend of materials and some specific factors that are unique to the OFET. The complexity and range of possible blend microstructures increases when compared to a single component film

<sup>a</sup>Centre for Plastic Electronics and Department of Physics, Imperial College London, South Kensington, SW7 2AZ, UK

<sup>b</sup>Department of Chemistry, Imperial College London, South Kensington, SW7 2AZ, UK

<sup>c</sup>Department of Materials, Imperial College London, South Kensington, SW7 2AZ, UK

† This paper is part of a themed issue of *Journal of Materials Chemistry* on Interface engineering of organic and molecular electronics, guest edited by Alex Jen.



Jeremy Smith

Jeremy Smith received his MSci degree in Materials Science from the University of Cambridge in 2007 and is currently studying for a PhD in the Physics department at Imperial College London. His research, under the supervision of Dr Thomas D. Anthopoulos, is focused on the development of high mobility organic field effect transistors (OFETs) with a particular interest in the links between thin-film morphology and

charge transport in both single devices and simple integrated circuits.



Thomas D. Anthopoulos

Thomas Anthopoulos is a Reader in Experimental Solid-State Physics in the Department of Physics at Imperial College London. He received his B.Eng., and Ph.D., from Staffordshire University in UK. In 2001 he moved to University of St. Andrews where he worked on dendrimer-based organic light-emitting diodes. In 2003 he joined Philips Research Laboratories in The Netherlands to work on ambipolar organic semiconductors, devices and integrated circuits. In 2005 he was awarded an EPSRC Advanced Fellowship and in 2007 a RCUK Fellowship both hosted in the Department of Physics, Imperial College. His research interest is focused on the physics of organics, metal oxides and hybrid semiconductors and devices (photograph courtesy of Ms Meilin Sancho).

and are dependent upon the rate of solvent evaporation during processing, solution viscosities, surface properties of the substrate, the degree of crystallinity of the individual components and the miscibility of the components. Solution processing allows the simple fabrication of blend films and is compatible with large scale, and potentially low cost, technologies such as dip-coating, spray coating, inkjet printing and gravure printing.<sup>7</sup> In addition a wide range of substrates can be utilised including flexible and transparent plastics.<sup>8</sup> However, it is a process that is often far from thermodynamic equilibrium and this can lead to interesting, if at times difficult to control, morphological features such as vertical phase separation. Also, unlike in a solar cell or OLED, conduction within an OFET occurs mainly in a quasi-two-dimensional fashion at the interface between the semiconductor and the dielectric layer, thus making it vital to be able to control the microstructure and composition at this location. Typically this accumulation layer will be <10 nm thick<sup>9</sup> with charge densities 3–4 orders of magnitude higher than in a diode structure.<sup>10</sup> Another aspect to consider in electronic devices is the percolation pathways for electrons or holes between electrodes. In many systems, especially polymer–polymer ones, phase separation due to the low entropy of mixing will occur and crystalline as well as amorphous regions may exist. Therefore charge conduction in a thin film can be highly non-uniform.<sup>11</sup>

The advantages of using a blend of materials for OFETs can, however, outweigh the extra complexity introduced. Three key areas in OFET research are the ability to produce high charge carrier mobility devices, the ability to have n- and p-type conduction with equally good performance for complementary logic circuits, and the simplification of the fabrication procedure for large area electronics. Intrinsically there are many organic materials, such as rubrene,<sup>12</sup> that have hole mobilities greater than amorphous silicon and are therefore potentially useful, however, forming uniform thin films, maintaining their performance over device lifetimes or creating an ambipolar molecule are not simple tasks. Chemical tailoring of molecules produces a wide range of properties allowing the optimisation of parameters such as solubility or air stability, however, blending materials sometimes offers a simpler or better alternative.

### 1.1 Organic transistor characterisation

The OFET is a thin film device that can be modelled in a similar fashion to its inorganic equivalent, allowing the field-effect charge carrier mobility to be calculated.<sup>13</sup> Schematics of typical devices are shown in Fig. 1. In general the current between source and drain electrodes,  $I_D$ , for a given applied gate voltage,  $V_G$ , and drain voltage,  $V_D$ , is given by,

$$I_D = \frac{W}{L} \mu C_i \left[ (V_G - V_T) V_D - \frac{V_D^2}{2} \right] \quad (1)$$

where  $W$  and  $L$  are the channel width and length respectively,  $\mu$  is the field-effect mobility,  $C_i$  is the geometric capacitance of the dielectric layer, and  $V_T$  is the threshold voltage. Most organic systems will deviate from this ideal due to the charge injection barrier (manifested as a contact resistance), electric field dependent mobilities, and the presence of charge trapping or donor states within the semiconductor. Despite this it is possible to

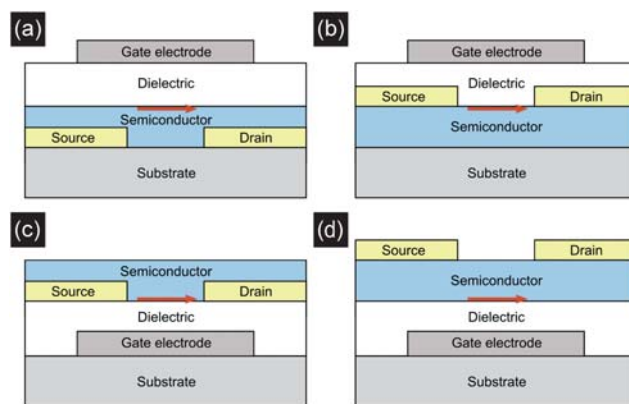


**Fig. 1** Schematic representations of field-effect transistor architectures, (a) top-gate bottom-contact, (b) top-gate top-contact, (c) bottom-gate bottom-contact, and (d) bottom-gate top-contact. The arrow shows the charge conduction interface.

extract a mobility in both the linear regime,  $V_D \ll (V_G - V_T)$ , and the saturation regime,  $V_D \geq (V_G - V_T)$ , of the OFET. These are given by the following equations:

$$\mu_{\text{lin}} = \frac{L}{WC_i V_D} \left( \frac{\partial I_{D \text{ lin}}}{\partial V_G} \right) \quad (2)$$

$$\mu_{\text{sat}} = \frac{L}{WC_i} \left( \frac{\partial^2 I_{D \text{ sat}}}{\partial V_G^2} \right) \quad (3)$$

### 1.2 Thin film morphology and phase separation

Two or more component films will often phase separate during the deposition process and this is particularly true for polymer–polymer blends. For such a system, assuming random polymer conformations, it is well established that the entropy of mixing per unit volume ( $\Delta S_{\text{mix}}$ ) can be approximated using a lattice model<sup>14</sup> and is given by,

$$\Delta S_{\text{mix}} = - R \left( \frac{\rho_1}{M_1} \phi_1 \ln \phi_1 + \frac{\rho_2}{M_2} \phi_2 \ln \phi_2 \right) \quad (4)$$

where  $\rho$ ,  $\phi$  and  $M$  refer to the density, volume fraction and molecular weight respectively of each polymer component and  $R$  is the molar gas constant. Therefore even for moderate molecular weight polymers, the contribution to the free energy change is negligible and is dominated by the enthalpy of mixing, or accordingly the interaction energy between the polymer chains.<sup>15</sup> Dispersive interactions are generally not sufficient for thermodynamically favourable polymer mixing and so liquid–liquid phase separation most often occurs. Entropic effects are more pronounced for small molecule–polymer or small molecule–small molecule systems and thus phases containing significant amounts of both components are common. However, solid–liquid and solid–solid phase separation can still occur in the form of crystalline molecular entities embedded in an amorphous or semi-crystalline matrix as described in Sections 3.2 and 3.3. In the latter case there will be contributions to  $\Delta S_{\text{mix}}$  from the effects of chain folding in the polymer crystallites.

The actual process of liquid–liquid phase separation during the formation of solid thin films from solution can occur by either spinodal decomposition<sup>16</sup> or by nucleation and growth.<sup>17</sup>

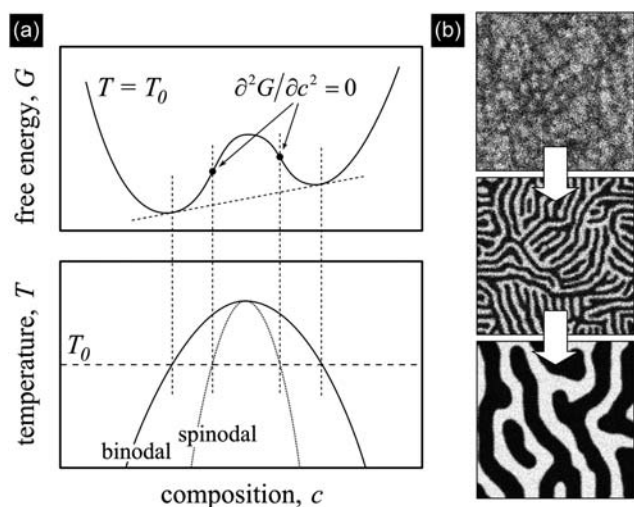


**Fig. 2** (a) Free energy of a binary system as a function of composition and the miscibility region showing the origin of the binodal and spinodal lines, and (b) typical evolution of a blend microstructure phase separating by spinodal decomposition.

In addition, subtle processing variations can result in vertical and/or lateral segregation on a variety of length scales. Spinodal decomposition in polymer–polymer blends has been shown to lead to both of these possibilities. A two component system with a composition,  $c$ , that is unstable to small fluctuations in concentration, in other words those where  $\partial^2 G/\partial c^2 < 0$  ( $G$  being the free energy), will spontaneously phase separate with the fluctuations increasing and coarsening over time (see Fig. 2). This type of process is common during spin coating due to the rapidity of solidification, thus preventing nucleation and growth by avoiding the binodal temperature/composition region. The wavelength of fluctuations both parallel,  $q_{\parallel}^{-1}$ , and perpendicular,  $q_{\perp}^{-1}$ , to the substrate surface are key to determining the final microstructure since thin film interfaces break the symmetry of the system.<sup>18</sup> Long wavelength fluctuations grow at the expense of small ones but are confined in the direction perpendicular to the surface. Therefore preferential attraction of one component to the substrate<sup>19</sup> or an increase in  $q_{\perp}^{-1}$  leads to a preference for vertical phase separation. It has also been shown by light scattering experiments during spin coating that a vertically segregated bilayer can form which then destabilises and forms lateral domains.<sup>20</sup> The evaporation rate and viscosity of the solution can be used to vary between such lateral and vertical separation.

The phase behaviour is, however, complicated by the fact that during solution processing of blends we must take into account at least three components including the solvent, and therefore must consider the ternary phase diagram. This has been done for example for a polymer(A)–polymer(B)–solvent system in relation to OLEDs<sup>21</sup> and is shown in Fig. 3. As the solvent evaporates the composition point shifts vertically towards the solid–solid axis passing from the single solution phase to the two phase region where A-rich : solvent and B-rich : solvent phases form. During this period there must be diffusion of A from the B-rich phase and *vice versa* and continued solvent evaporation leading to an increased solute concentration and increased solution viscosity. Thus we must not only consider the miscibility of the two components being blended but also their miscibility with the

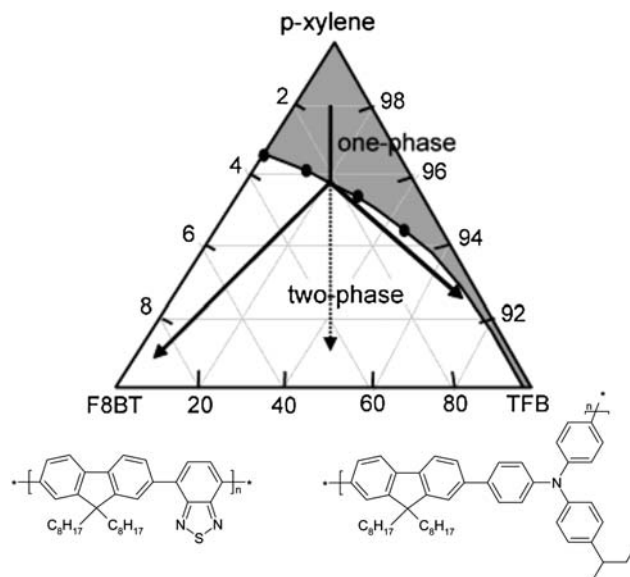


**Fig. 3** A ternary phase diagram (at  $T = 22\text{ }^{\circ}\text{C}$ ) for the p-xylene:F8BT:TFB blend system and their chemical structures, showing the process of solvent evaporation and phase separation. Adopted from ref. 21 (reproduced by permission of the American Chemical Society).

solvent, *i.e.* their solubility. Systems and thin film microstructures may thence be dominated by the solvent–solute or the solute–solute<sup>22</sup> interactions. Examples of both are shown schematically in Fig. 4. In the former case evaporation of solvent from the top surface leads to a higher solute concentration and therefore preferential accumulation of the more soluble component at this interface.<sup>23</sup> This concentration gradient affects the spinodal decomposition and leads to a vertically segregated film. In the latter case the order in which the two components solidify affects the microstructure and the solvent evaporation less strongly affects the liquid–liquid phase separation. For example the first component to solidify may be expelled to the interfaces as the second solidifies. Controlling the processing temperature in crystalline–crystalline polymer blends, for instance, lets one choose which component crystallises first hence, as we will see in Section 3.1, allowing optimisation of the structure and properties of the semiconducting material. If the second material is

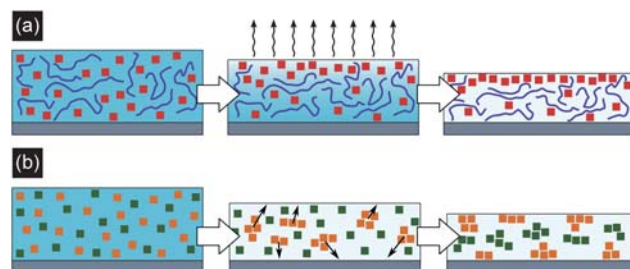


**Fig. 4** Two schematic example representations of vertical phase separation. (a) The solvent evaporation leads to a concentration gradient with the more soluble component (red squares) moving to the top surface. (b) Crystallisation-induced phase separation whereby the order of crystallisation of the two solute components determines the microstructure. In this case the first to solidify (orange squares) is expelled to the interface as the second crystallises.



crystalline there can be an enthalpic driving force for solid–liquid phase separation, whereas an amorphous material may interact more strongly with the initial component thus reducing the amount of segregation in the final solidified microstructure. In eutectic (crystalline–crystalline) systems the composition will affect which material solidifies first. At the eutectic composition,  $c_{\text{eutectic}}$ , both components solidify at the same time and produce a very fine scale microstructure; on either side of this composition coarser microstructures are formed with one phase partially solidifying, in the form of primary crystals, before the remaining eutectic mixture.<sup>24</sup>

As well as the phase separation of the blend components, it is usually important to control their degree of crystallinity (when dealing with crystallisable species). Although there are some relatively high mobility amorphous materials,<sup>25</sup> introducing some crystallinity, either as semi-crystalline polymers<sup>1</sup> or small molecular materials,<sup>26</sup> tends to lead to increased  $\pi$ -orbital overlap, more electronic delocalisation and higher mobilities. Sufficient time for crystallisation during processing or annealing after film formation is usually needed for high crystalline order.<sup>27</sup> Most thin film devices, either based on small molecules or polymers, or mixtures thereof, will be polycrystalline in the former case or semi-crystalline in the latter, with often randomly orientated crystal directions in the plane of the film. This assumes there has been no attempt at alignment by, for example directional solidification or substrate treatment or patterning.<sup>28</sup> In the case of OFETs it is useful to have the highest mobility in the direction of transport along the channel. Within a blend one component may disrupt the crystal structure or grain/spherulite structure of a particular phase especially if there is significant miscibility of the components.<sup>29</sup> However, the advantages of blending highly crystalline materials to improve mechanical characteristics and the possibility to control where crystallisation occurs in a thin film generally outweigh any disorder created in the crystal structure.

## 2. Ambipolar and n-type blends

Having both n- and p-type organic materials<sup>30</sup> is vital for many applications since it becomes possible to fabricate complementary<sup>31</sup> or complementary-like logic.<sup>32,33</sup> Compared to unipolar logic using only a p-type semiconductor, complementary logic is more efficient and reliable since power is only dissipated during switching and noise margins are generally larger. However, high mobility n-type organic devices are rare due to the problems of electron trapping within the OFET<sup>34</sup> and air stability issues are often present because of their high HOMO levels.<sup>35</sup> Also there are advantages to using an ambipolar system during solution processing, again not common, since this negates the need for semiconductor patterning. Blends have been used to address some of these problems with the combination n-type and p-type components being an early and frequent area of research.

One of the first examples of a solution-processed ambipolar OFET system was described by Geens *et al.*<sup>36</sup> A blend of 6,6-phenyl- $C_{61}$ -butyric acid methyl ester (PCBM) and poly-(2-methoxy-5-(3',7'-dimethyloctyloxy)-*p*-phenylene vinylene) (MDMO-PPV) were used as n- and p-type materials respectively. High levels of PCBM in the blend were needed to obtain good electron conduction, however, this did not reduce the hole

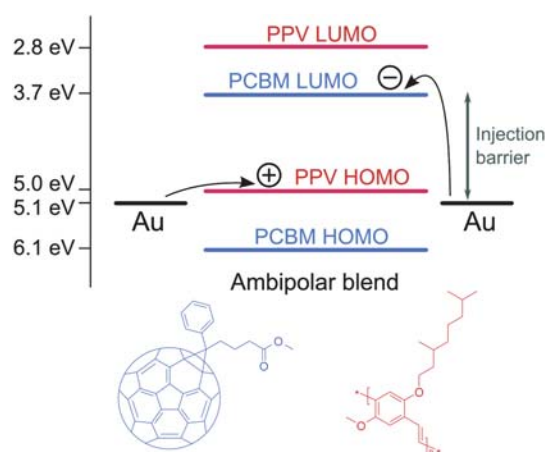


**Fig. 5** The energy levels within a PCBM : MDMO-PPV blend for ambipolar OFETs and the chemical structures of the two materials. The large injection barrier for electrons from gold electrodes into the PCBM LUMO is clear but in reality is reduced by band bending due to PCBM–Au interactions.

mobility in the MDMO-PPV. This is explained by PCBM-rich clusters that do not form percolation pathways at low fullerene concentrations. Meijer *et al.*<sup>32</sup> used the same system to demonstrate that ambipolar blend OFETs can be integrated to construct simple complementary-like inverter logic circuits. More recently ambipolarity, with a low activation energy for charge transport as a function of temperature, was achieved using poly(2-methoxy-5-(2'-ethylhexyloxy)-*p*-phenylene vinylene) (MEH-PPV) but with  $C_{60}$  as the n-type material demonstrating the increased processability possible when using a blend.<sup>37</sup> The formation of an interpenetrating network of the two components by selecting a suitable composition allowed percolation pathways for electrons and holes. However, one of the major issues becomes the injection of carriers due to the position of the work function of the electrodes with respect to the MDMO-PPV HOMO level and the PCBM LUMO level as shown in Fig. 5. Electron injection into PCBM from gold has a considerable associated energy barrier but is reduced to  $\sim 0.76$  eV assuming an interfacial dipole interaction. Pure PCBM films showed an electron mobility two orders of magnitude higher than when used in the blend, unlike PPV which was largely unaffected by blending. This suggests an important feature in blend OFETs namely that wetting of a particular phase on the substrate or the contacts (as in this case) is often needed for good electrical performance. Three component blends of PCBM : MDMO-PPV : poly(9,9-dioctylfluorene) (in the ratio 2 : 1 : 1) have also been used for ambipolar OFETs on various polymer dielectrics.<sup>38</sup> The dielectric surface here plays a key role in determining the semiconductor morphology and hence the electrical properties. Large-scale phase separation with  $\sim 200$  nm domains led to only unipolar transport, however, a more interconnected microstructure with fewer isolated domains resulted in ambipolar OFETs.

Poly(3-hexylthiophene) (P3HT) was also found to be a suitable substitute for the hole transporting material and similar studies have been carried out using PCBM : P3HT blends,<sup>32,39,40</sup> especially since they have potential importance in solar cell applications. It has been shown that measured mobilities decrease for both components in such a blend;<sup>39</sup> this may be due to a decrease in effective channel width since only part of the film is

contributing to each type of conduction, however, electron mobility falls much more dramatically than hole mobility. The effect of contact wetting was removed in this study by using a top-contact OFET architecture and in addition contact resistance effects caused by energy level mismatch were accounted for. Despite this a considerable improvement in electron mobility, but not hole mobility, was observed by annealing the films. This can be attributed to a change in morphology that is also seen in solar cells, whereby the PCBM aggregates into clusters. Several groups<sup>41</sup> have reported that these PCBM-rich regions may vertically phase separate which can be advantageous in n-type OFETs if there is an increase in concentration at the dielectric interface. The complexities of polymer–fullerene microstructures with relation to solar cells are beyond the scope of this review but have been well described by Hoppe.<sup>5</sup>

Another n-type material that has been employed in blends is poly(benzo bisimidazobenzophenanthraline) (BBL). When blended with the p-type small molecule copper phthalocyanine (CuPc), air stable ambipolar devices are obtainable but are critically dependent on the phase separated microstructure and CuPc polymorph produced.<sup>42</sup> Additionally measured mobilities are lower than the single component films. The devices were either treated to remove the solvent with water or methanol which led to two distinct CuPc crystallite shapes. Electron conduction through the polycrystalline BBL was seen in both cases, however, only when treated with methanol was any hole conduction measured due to the formation of large plate-like CuPc domains. Once again this highlights the need for conduction pathways controlled by phase separation. BBL has been used in a purely electron conducting blend with the polymer poly(*p*-phenylene-2,6-benzobisthiazole) (PBZT).<sup>43</sup> As the concentration of BBL is reduced, a step-like dependence of OFET mobility was observed. Between 5–60 wt% PBZT there was an approximately constant electron mobility of  $5 \times 10^{-5} \text{ cm}^2/\text{V s}$  and a higher current on/off ratio than in either of the parent polymers. Above 60 wt% PBZT mobility dropped exponentially with concentration which further supports the concept of percolation behaviour. In the constant mobility regime it is suggested that increased disorder has little influence on the electrical properties due to the phase separation effect.

In summary for ambipolar transport it is vital to ensure that conduction at the dielectric interface and from contacts to semiconductor is possible. This has been achieved by producing the optimal phase separated morphology and controlling the wetting of both components on the substrate and metal. However, in terms of electron and hole device mobilities it is difficult to prevent a loss of performance when blending compared to the pristine component films.

### 3. Blends for high charge carrier mobility devices

There is considerable focus on increasing charge carrier mobilities in OFETs especially to compete with current inorganic thin film technologies such as amorphous silicon. For active-matrix organic light emitting diode (AM-OLED) display applications, high currents are needed to drive the OLED therefore higher mobility materials mean that the transistor circuitry can be smaller compared to the pixel size. In addition it is required to have reproducible performance over the entire substrate for

integrated circuits to function reliably. Methods for improving mobility that have been used for single component systems tend to involve increasing the solubility of crystalline small molecular materials to make them more processable, or increasing the crystallinity of polymers by for example using a liquid-crystalline phase<sup>44</sup> or more regioregular molecules.<sup>45</sup> Recently several techniques using blended materials have been used to combine high carrier mobilities with features such as ease of processing, film uniformity, environmental stability and enhanced mechanical properties.

#### 3.1 Crystallisation control within blend films

Highly crystalline materials are often also hard to process from solution due to the rate at which the crystals form leaving an incomplete or anisotropic thin film. Being able to control this crystallisation is important and has been achieved in several ways including the use of a vitrifying component to delay crystallisation until after film formation<sup>46</sup> and the use of enhanced phase separation within crystalline-crystalline polymer blends.<sup>47</sup>

Goffri *et al.*<sup>47</sup> have studied the use of semi-crystalline regioregular poly(3-hexylthiophene) (P3HT) with several common bulk polymers, poly(styrene)s (PS) and poly(ethylene)s (PE), that are low cost and have good mechanical properties. A comparison was made between using amorphous and crystalline polymers for this purpose, and specifically how the limit of percolation for electrical conduction was affected. The advantage of using a crystalline–crystalline system is that, provided one can control which component crystallises first, crystallisation-induced phase separation can lead to a high degree of vertical segregation. It was observed that it is possible to have P3HT concentrations as low as 3 wt% in the bulk but still have sufficient material for percolation at the semiconductor–dielectric interface.

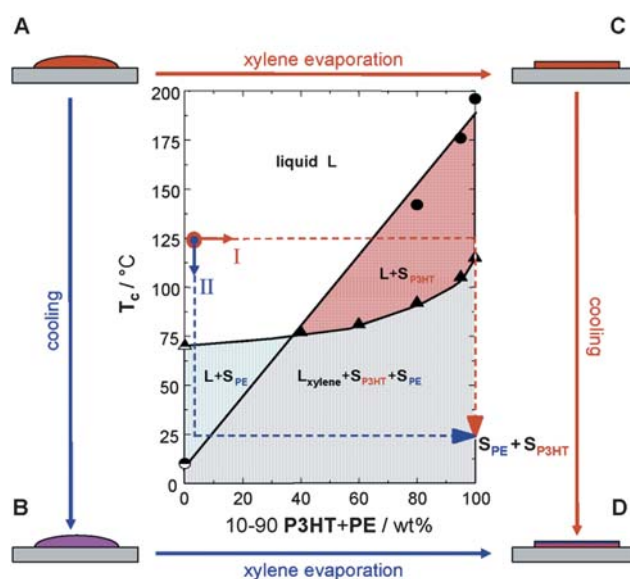


**Fig. 6** Phase diagram of a P3HT:PE:xylene blend where the ratio of P3HT to PE is fixed at 1 : 9. Schemes I and II show two possible routes for film formation, firstly solvent evaporation at high temperature and then solidification, and secondly cooling to room temperature before removal of the solvent. Adopted from ref. 47 (reproduced by permission of the Nature Publishing Group).

For comparison, using an amorphous polymer leads to a steady degradation of OFET performance with decreasing P3HT concentration. Critically the P3HT must crystallise before the second component, and low evaporation and cooling rates during film processing are needed in order to obtain the optimum morphology and prevent quenching into a disordered amorphous state. The former is possible by allowing solvent evaporation to occur above the insulating polymer's melting temperature driving the system into the liquid–solid P3HT phase region (see scheme I Fig. 6), before allowing the sample to cool and the second polymer, here PE, to crystallise. Phase separation in the liquid state as well as during the second crystallisation occurs leading to substantial accretion of P3HT at the film interfaces.

Alternatively, an amorphous film can be first formed from solution and then subsequently crystallised by annealing. This removes the need to consider the kinetics of spin coating or other solvent evaporation processes. One way to do this has been demonstrated by Stingelin-Stutzmann *et al.*<sup>46</sup> and involves the addition of a glass-inducing species to rubrene with a minor amount of atactic PS to improve mechanical film properties. Rubrene is an excellent organic semiconductor and in single crystal form has demonstrated mobilities up to  $20 \text{ cm}^2/\text{V s}$ .<sup>12</sup> By the addition of the similar molecule, diphenylanthracene, a glassy phase is readily formed between 20–40 mol% rubrene when

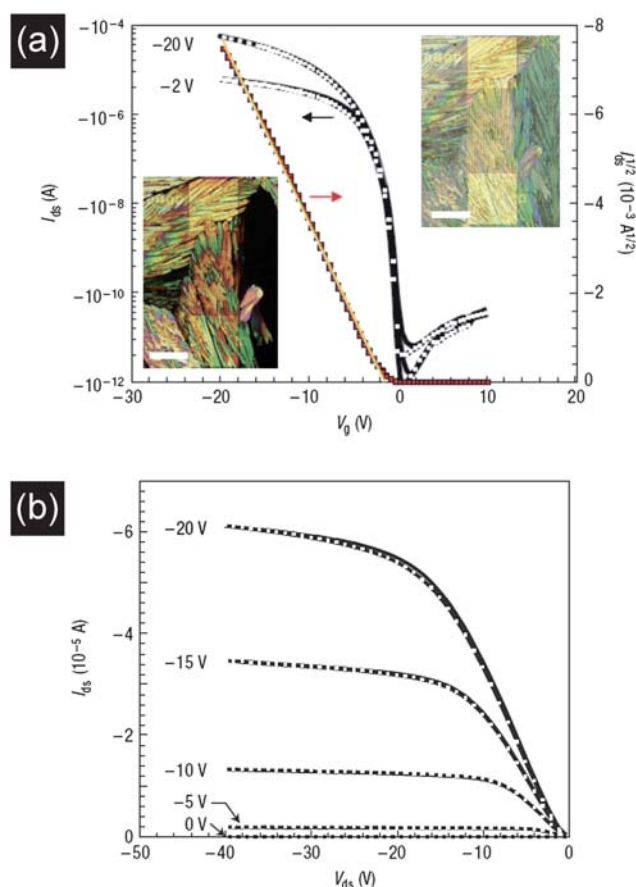


**Fig. 7** (a) Transfer and (b) output characteristics of a rubrene:diphenylanthracene transistor after crystallisation at  $T_{\text{eutectic}} < T < T_m$ . Inset to (a) are polarised and non-polarised light microscopy images of the film showing large, highly crystalline grains (scale bar  $150 \mu\text{m}$ ). Adopted from ref. 46 (reproduced by permission of the Nature Publishing Group).

cooling from the melt. This disordered phase can then be converted to a crystalline, active material by annealing above the eutectic temperature but below  $T_m$ , and resulted in OFETs with mobilities of  $0.7 \text{ cm}^2/\text{V s}$  (Fig. 7). By selecting a hypereutectic, rubrene-rich composition the annealing stage leads to melting and recrystallisation of the rubrene phase into a planar polycrystalline structure with  $a,b$ -planes parallel to the substrate surface and large, birefringent grains. Annealing above  $T_m$  or below  $T_{\text{eutectic}}$  resulted in less well ordered films and lower OFET mobilities. The phase diagram showing this particular system is given in Fig. 8.

### 3.2 Oligothiophene–polymer blends

Adding polymers to small molecule species that are difficult to process is a common technique to improve film forming properties. The higher viscosity of polymer solutions and their lower propensity to crystallise produces a more uniform thin film,

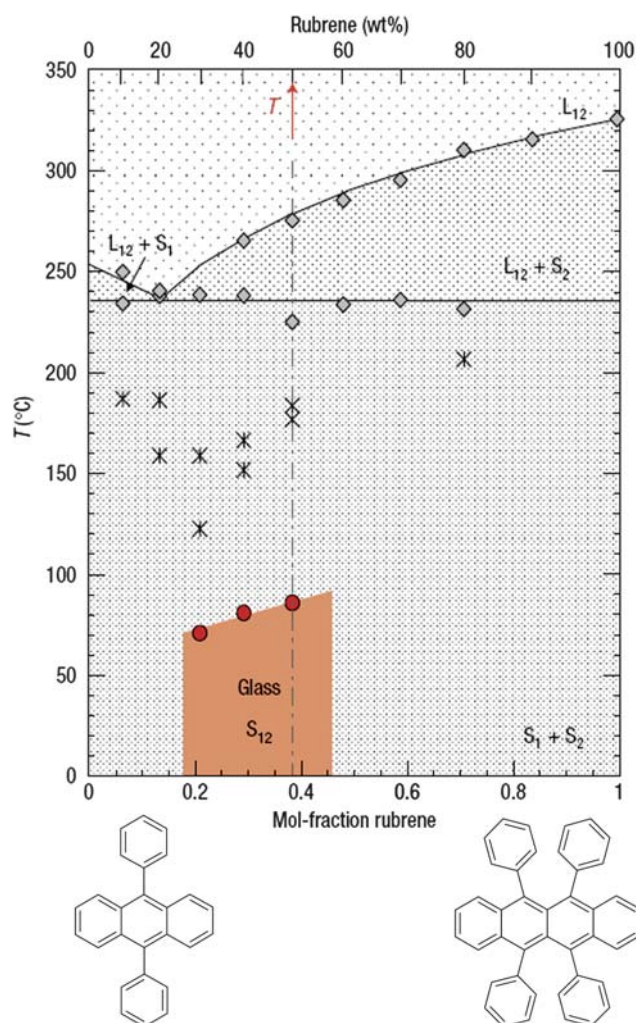


**Fig. 8** Binary phase diagram of the rubrene : diphenylanthracene system and their chemical structures. The data points were measured from DSC heating curves with red symbols being the glass transition temperature, crosses being crystallisation temperatures and grey symbols being melting and eutectic temperatures. The dashed line represents a typical composition used for vitreous solution processed OFETs. Adopted from ref. 46 (reproduced by permission of the Nature Publishing Group).



however, in general they have carrier mobilities that are 1–2 orders of magnitude lower than the best small molecules. Oligothiophene molecules<sup>48</sup> including  $\alpha$ -sexithiophene have been widely studied for high mobility OFETs both as thermally evaporated and solution-processed films. The latter generally involves the addition of solubilising alkyl chains to the terminating thiophene rings a common example being  $\alpha,\omega$ -dihexylquaterthiophene (DH4T). However, increased solubility generally also leads to a more disrupted crystal structure due to the flexible side chains. Blending these molecules with polymers offers the potential to combine the advantageous properties of both.

Russell *et al.*<sup>49</sup> first reported DH4T blends with P3HT for OFETs realising mobilities of up to 0.01 cm<sup>2</sup>/V s, however this was strongly limited by the low P3HT mobility. The change in mobility with DH4T concentration was modelled by a saturation process with a critical concentration of 29 wt% and an order of magnitude increase in mobility when moving from 10 to 50 wt% DH4T. Below the critical concentration there is only slight agglomeration of material but at higher concentrations well-defined, micron sized, DH4T-rich crystallites embedded in the bulk film are observed (Fig. 9). The performance of these devices clearly depends upon percolation pathways within the channel and the ability to inject carriers into each of the two phases. From the output characteristics there is non-linearity for low source–drain voltages. Also at these voltages the current does not differ a great deal from the pure P3HT OFET suggesting that there is a significant energy barrier to injection into the high mobility, DH4T-rich pathways. However, at higher values of  $V_D$  conduction through these pathways becomes more viable and high mobilities are measured. The mobility can be modelled simply using a percolation analysis based upon a high mobility ( $\mu_H$ ) and low mobility

( $\mu_L$ ) phase with a volume fraction,  $f$ , of the latter. In this case the mobility of a particular pathway is given by,<sup>50</sup>

$$\mu_{\text{path}}(f) = \frac{\mu_H}{1 + f \left( \frac{\mu_H}{\mu_L} - 1 \right)} \approx \frac{\mu_H}{1 + f \left( \frac{\mu_H}{\mu_L} \right)} \quad (\text{for } \mu_H \gg \mu_L) \quad (5)$$

Different pathways will have different values of  $f$  and OFET mobility will be dominated by the few with low  $f$  or the DH4T-rich regions in this case. However, by increasing  $\mu_L$  for a fixed  $\mu_H$  large changes in  $\mu_{\text{path}}$ , and therefore the overall mobility, can be achieved. Hence the importance of the P3HT performance as well as formation of the highly crystalline regions. DH4T has also been used in blends with poly(9,9-dioctylfluorene-*alt*-bithiophene) (F8T2) again dramatically improving the performance of OFETs when compared to the unblended polymer.<sup>51</sup> They also found that the polymer plays a key role in such blends, that the correct morphology, dependent on the blend composition, is needed and that the hole injection into the oligomer must be suitable for good electronic performance.

As stated above, one aim of blend semiconductors is to make small molecules easier to process and improve the mechanical properties of the resulting films. With this in mind Wolfer *et al.*<sup>52</sup> have shown that  $\alpha$ -quaterthiophene (4T), even without the solubilising alkyl chains of DH4T, can be blended with high-density poly(ethylene) (HDPE) to make solution processable OFETs without loss of electrical properties. The use of an insulating polymer indicates that by carefully controlling the crystallisation of the film it is not always necessary to have a relatively high mobility polymer matrix. Also a very low critical concentration of 4T was possible ( $\sim 10$  wt%) before OFET mobilities started to rapidly decrease. This effect is attributed to crystallisation-induced phase separation as seen in the crystalline polymer–polymer blends<sup>47</sup> discussed earlier. Again the critical concentration for conduction corresponds to the point of liquid miscibility, however, in this case the 4T always crystallises before the polymer which is favourable for OFET applications. Thus it was possible to study the effect of processing conditions on morphology and electronic properties of the film. Rapid removal of solvent at 130 °C followed by solidification was compared to cooling and evaporation of solvent at room temperature. The former yielded a much finer microstructure and a more uniform distribution of 4T crystallites. Also two different polymorphs of 4T were produced (as determined by wide-angle X-ray diffraction) dependent on the crystallisation temperature, but this is less likely to affect the charge transport. OFET mobilities of  $\sim 10^{-4}$  cm<sup>2</sup>/V s were measured when films were crystallised at 130 °C and when 4T concentrations were large enough ( $>10$  wt%) to induce liquid–liquid phase separation, otherwise values of  $\sim 10^{-6}$  cm<sup>2</sup>/V s with larger threshold voltages were obtained. This higher mobility is comparable to vapour deposited 4T on SiO<sub>2</sub><sup>53</sup> and demonstrates that it is possible, by ensuring suitable crystallisation of the semiconductor, to fabricate solution processable OFETs with normally difficult to process oligomers.

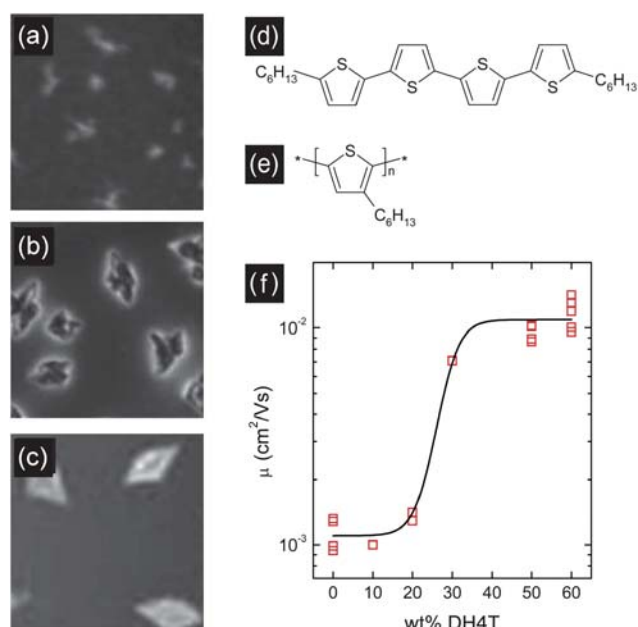


**Fig. 9** Optical micrographs of DH4T:P3HT blend films with (a) 20 wt%, (b) 30 wt%, and (c) 100 wt% DH4T. Chemical structures of (d) DH4T and (e) P3HT. (f) Mobility as a function of DH4T concentration fitted using a saturation model with a critical concentration of 29 wt%. Adopted from ref. 49 (reproduced by permission of the American Institute of Physics).

### 3.3 Acene–polymer blends

We will now examine a particularly successful group of blend systems involving high mobility, small molecular, acene-based

materials blended with amorphous (or sometimes semi-crystalline) polymers. These blends again combine the good semi-conducting properties of small molecules with the ease of processing and film uniformity of polymers. Furthermore there is a degree of microstructural control by vertical phase separation which can be used to preferentially crystallise the acene at the semiconductor–dielectric interface and hence give very high performance OFETs.

Pentacene has been investigated thoroughly as a high mobility material,<sup>54</sup> however, it is not readily solution processable except under relatively extreme conditions.<sup>55</sup> Recently several soluble derivatives developed by Anthony and coworkers have been used successfully as organic semiconductors, the two most common being 6,13-bis(triisopropylsilyl)ethynyl pentacene (TIPS-pentacene)<sup>56</sup> and 2,8-difluoro-5,11-bis(triethylsilyl)ethynyl anthradithiophene (diF-TESADT).<sup>57</sup> These materials have high intrinsic mobilities ( $>1 \text{ cm}^2/\text{Vs}$ ) however, solution processing can be made easier and lead to more uniform films if they are blended with a polymer without any loss, and sometimes with an improvement, in OFET characteristics. Such concepts were first reported in the patent literature<sup>58</sup> and then Hamilton *et al.* demonstrated devices with diF-TESADT : poly(triarylamine) (PTAA) blends showing very high mobilities for a solution processed film of up to  $2.4 \text{ cm}^2/\text{Vs}$  (Fig. 10).<sup>59</sup>

TIPS-pentacene blended with an insulating polymer has been shown to give good OFET performance and has been studied by several groups to better understand the materials system. Vertical phase separation is key to the high mobilities reported with the

aim being to produce an increased concentration of acene molecules at the conducting interface. Dual-gate OFETs, *i.e.* those with both a top- and bottom-gate, are a useful probe of interface properties since both channels can be measured within a single device. It has been shown that in a dual-gate OFET the top-gate shows better performance than the bottom in terms of mobility, threshold voltage and hysteresis.<sup>59</sup> This suggests that in this case the TIPS-pentacene-rich phase segregates to the upper interface and has been further confirmed by secondary ion mass spectrometry (SIMS) data. Using this technique<sup>60</sup> it is possible to measure elements as a function of depth in the film by ion milling at a known rate. Ohe *et al.*<sup>61</sup> report SIMS results that show TIPS-pentacene accumulation at both interfaces in the film signifying that the exact nature of the substrate critically affects the phase separation that occurs. Both of these results using SIMS are shown in Fig. 11. By changing the surface energy of the substrate it is possible to alter the performance of the transistor even if this is not the interface at which charge accumulation occurs and hence a morphological change must be occurring.<sup>62</sup> Similarly for TESADT : poly(methyl methacrylate) blends,<sup>63</sup> X-ray photo-emission spectroscopy combined with argon milling has recently been used to show that vertical separation occurs and can be enhanced by vapour annealing which improves acene diffusion and crystallisation. In addition high performance circuits have been fabricated with a diF-TESADT : PTAA blend despite using a bottom-gate, bottom-contact architecture.<sup>64</sup> Ring oscillators with fast stage delays ( $\sim 712 \text{ ns}$ ) suggest that the hole mobilities are high in these devices. Therefore it is proposed that the lower surface energy of the polymer dielectric substrate layer employed increases segregation to the bottom interface and improves the bottom channel performance. During spin coating, high boiling point solvents tend to be used to reduce evaporation rates and allow time for vertical phase separation to occur. Consequently there may be the formation of a wetting layer at the substrate interface due to a decrease in solvent concentration at the top interface. Surface energies of components and substrate, as well as the fact that the small acene molecules will diffuse faster than the polymer, will then play a key role in determining the vertical composition profile.

Kang *et al.*<sup>65</sup> have used neutron reflectivity (NR) and grazing incident X-ray diffraction (GIXD) measurements on deuterated-TIPS-pentacene : poly( $\alpha$ -methyl styrene) (P $\alpha$ MS) films to study both phase separation and crystalline orientation respectively.

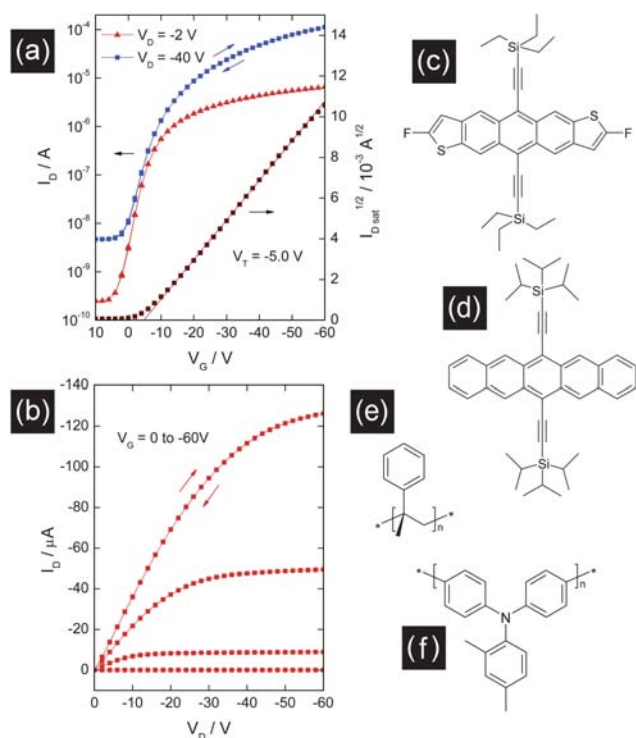


**Fig. 10** (a) Transfer and (b) output characteristics of a high mobility ( $>2 \text{ cm}^2/\text{Vs}$ ) OFET using a diF-TESADT:PTAA blend film. Chemical structures of (c) diF-TESADT, (d) TIPS-pentacene, (e) P $\alpha$ MS, and (f) PTAA. Adopted from ref. 59 (Copyright Wiley-VCH Verlag GmbH & Co. KGaA. Reproduced with permission).

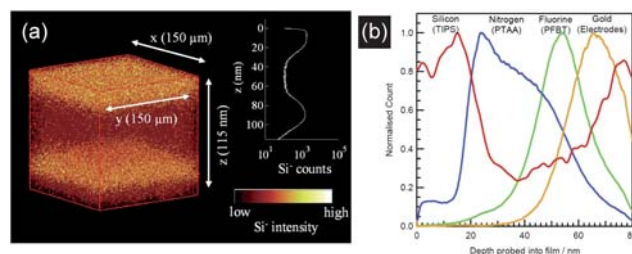


**Fig. 11** SIMS data for TIPS-pentacene blend films with the Si signal indicating the presence of the TIPS group, (a) shows accumulation at both interfaces compared to only the top surface in (b). Adopted from ref. 61 (reproduced by permission of the American Institute of Physics) and ref. 59 (Copyright Wiley-VCH Verlag GmbH & Co. KGaA. Reproduced with permission), respectively.



It was found that a low molecular weight PzMS only showed vertical phase separation after annealing above the glass transition temperature,  $T_g$ , however, the high molecular weight version always led to phase separation and annealing had very little effect (see Fig. 12 for NR results). Again vertical separation to both interfaces occurred in the latter case making bottom-gate OFETs a possibility. Uniform and stable devices with mobilities up to  $0.3 \text{ cm}^2/\text{V s}$  were fabricated. These effects are firstly a consequence of the lower  $T_g$  and secondly the increased entropy of mixing for lower molecular weight polymers. GIXD results showed that after phase separation there is a highly crystalline film with the (001) planes parallel to the substrate surface. This is the ideal orientation<sup>66</sup> for high mobility devices as it puts the  $\pi$ -stacking in the direction of charge transport.

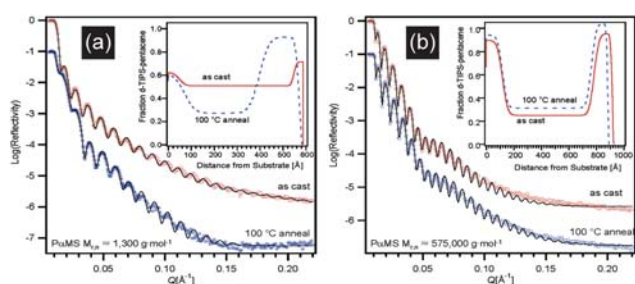


**Fig. 12** Neutron reflectivity measurements on deuterated-TIPS-pentacene:PzMS blends and the calculated vertical distribution of the TIPS-pentacene for PzMS molecular weights of (a)  $1.3 \text{ kg mol}^{-1}$  and (b)  $575 \text{ kg mol}^{-1}$ . Both as cast films and those after annealing at  $100^\circ\text{C}$  are shown. Adopted from ref. 65 (reproduced by permission of the American Chemical Society).

The polymer matrix employed plays an important role in film morphology and electrical properties. Initial experiments using insulating polymers such as PzMS fulfilled the need for mechanical and thin film forming properties, however, by moving to a semiconducting polymer such as PTAA, which is still amorphous, an improvement in OFET mobility could be achieved ( $0.69 \text{ cm}^2/\text{V s}$  compared to  $1.1 \text{ cm}^2/\text{V s}$  for TIPS-pentacene<sup>59</sup>). This can be explained by the improved conduction pathways between acene-rich regions provided by the polymer and the enhanced injection into the PTAA from the gold contacts. The same improvement was seen in bottom-gate devices,<sup>67</sup> with insulating polymer blends having  $4\text{--}5\times$  lower mobilities than PTAA blends. The effect of morphology on devices has been explored by Madec *et al.*<sup>68</sup> and a comparison made between the use of semi-crystalline and amorphous polymers. It was observed that the use of PzMS led to an accumulation of the TIPS-pentacene on the top surface but only when the overall the acene concentration was  $>40\text{--}50 \text{ wt}\%$ , and using amorphous poly(styrene) led to no vertical phase separation at all (Fig. 13). Low concentrations of TIPS-pentacene in an amorphous polymer meant that during film formation, liquid-liquid phase separation was not pronounced, small crystallites dispersed in a continuous polymer matrix were produced and OFETs had low measured mobilities. Clearly for higher acene concentrations, dependent on the polymer matrix and processing conditions, it is possible to obtain vertical segregation and high hole mobility. However, by using a semi-crystalline polymer (such as isotactic poly(styrene)) it was shown that vertical phase separation to both top and bottom interfaces could be achieved over a wide range of compositions even down to  $10 \text{ wt}\%$ .

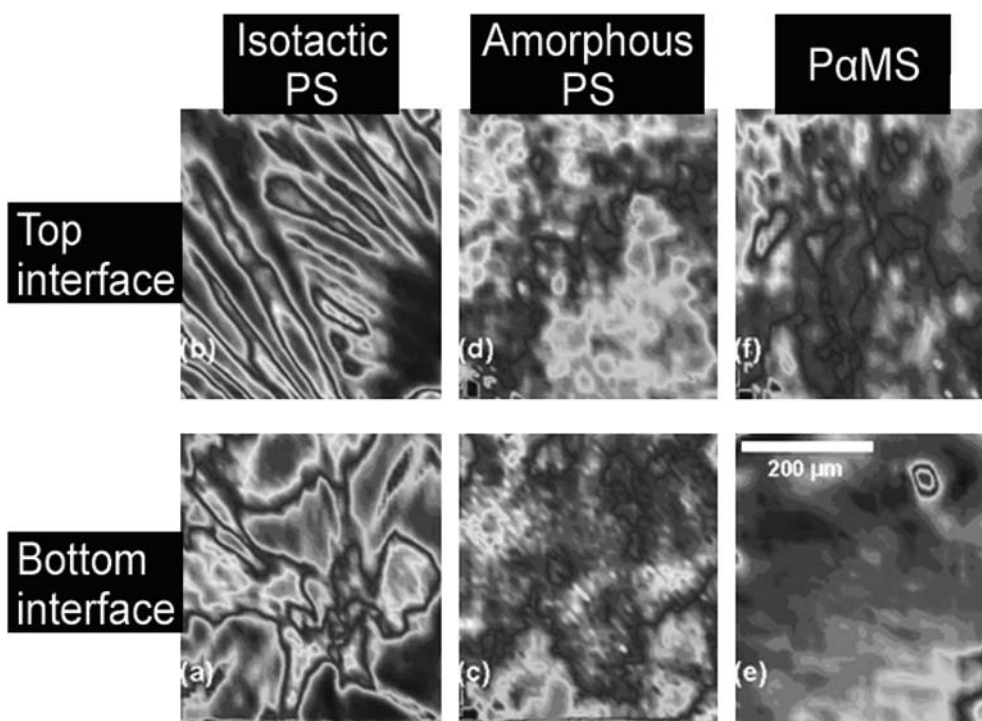


**Fig. 13** Infrared spectroscopy images of blend films showing absorbance at  $2130 \text{ cm}^{-1}$  (stretching band in TIPS-pentacene). Films consist of TIPS-pentacene and either isotactic PS, amorphous PS or PzMS. Both the top and bottom surfaces of the thin film are imaged, demonstrating interface enrichment of TIPS-pentacene due to vertical phase separation in the cases of (a), (b) and (f). Adopted from ref. 68 (reproduced by permission of The Royal Society of Chemistry).

TIPS–pentacene. This corroborates well with the results of crystalline–crystalline blend phase separation as discussed in Section 3.1. Therefore, overall a suitable substrate surface energy and a long enough time for diffusion of the acene-rich phase to the interface, as well as crystallisation of this phase, appear to be just as vital as the intrinsic electrical properties of the film components for good device performance.

## 4. Blends for OFET self-assembly and patterning

It is possible to use blended materials to aid the processing of OFETs and circuits for their intended large-scale applications. Self-organisation of the two components has the potential to allow formation of gate dielectric and semiconductor in a single step, the localisation of one component in the OFET channel, or the self-encapsulation of organic circuitry. These techniques can potentially reduce the cost of fabrication which is one of the key advantages of using organic materials.

### 4.1 Gate dielectric self-formation

Blending the semiconductor and dielectric, in the case where significant vertical phase separation occurs, allows formation of a bilayer suitable for OFETs. One of the first demonstrations of this technique used a poly(9,9-dialkylfluorene-*alt*-triarylamine) (TFB) blended with the cross-linkable dielectric divinyl-tetramethyldisiloxane-bis(benzocyclobutene) (BCB) in 1,3,5-trimethylbenzene.<sup>69</sup> Due to the large interaction parameter between TFB and BCB, caused in part by the siloxane group in the BCB, complete phase separation occurs during film formation. Controlling the rate of solvent evaporation by altering the solvent vapour pressure during spin coating and selecting a composition that will lead to spinodal decomposition produced a vertically separated bilayer with BCB on the top surface. Several factors contribute to making this system suitable for OFET applications. Firstly the degree of the phase separation produces both negligible intermixing within the phases and a very abrupt interface (estimated to be  $\sim 4$  Å wide) between the phases. Secondly there are no –OH groups and a low chance of other impurities acting as charge trapping sites during conduction at the interface. Finally the BCB dielectric layer was found to be free of pin-hole defects that would increase gate leakage. However, interface roughness, controlled by the solvent evaporation rate, had to be minimised in order to reduce charge trapping or scattering and obtain devices only limited by the mobility of the TFB and contact resistances.

A similar system but for bottom-gate OFETs was demonstrated by Chung *et al.* in which F8T2 was employed as the semiconductor and thermally curable dimethylsiloxane (DMS) as the insulator.<sup>70</sup> Upon heating DMS at 120 °C conversion to the hydrophobic rubber poly(dimethylsiloxane) (PDMS) occurs. During spin coating DMS preferentially phase separates to the SiO<sub>2</sub> substrate. Also during the thermal curing stage further segregation of the components takes place, facilitated by the low glass transition temperature of PDMS, leading to some accumulation of PDMS on the top surface which is advantageous as it encapsulates the OFET. The lower layer of PDMS then acts as a treatment for the SiO<sub>2</sub> gate dielectric rather than the gate itself, however, the performance of such devices was higher than pure

F8T2 on octadecyltrichlorosilane (OTS) treated SiO<sub>2</sub>. A negative correlation between surface energy of the dielectric and OFET mobility was observed for three different semiconducting polymers and additionally has been noted by other groups.<sup>71</sup> However, solution processing on a low surface energy substrate without de-wetting can be challenging. Therefore the use of a blend allows the formation of a good semiconductor–dielectric interface on a variety of substrates. Simple polymer dielectrics that do not need thermal cross-linking can also be processed in this way. Vertically segregated P3HT : poly(methyl methacrylate) (PMMA) blends have been used for OFETs<sup>72</sup> with the PMMA either operating as a dielectric treatment or as the dielectric itself. The high surface energy of the substrate in this case leads to preferential formation of PMMA on the lower surface and, as with previously discussed polymer–polymer blends (Section 3.1), P3HT concentration can be reduced to  $\sim 5$  wt% whilst still retaining electrical conduction. Low voltage operation of OFETs also becomes possible with systems such as this since the thickness of the dielectric can be very small and hence its geometric capacitance will be high. Small molecular semiconductors can also be used in place of polymers for example the TESADT : PMMA blend.<sup>63</sup> Solvent annealing in this case was used to enhance the vertical phase separation and allow crystallisation of the TESADT on the top surface producing a bilayer with very low concentrations of small molecule in the PMMA dielectric. High mobility (up to 0.47 cm<sup>2</sup>/V s) OFETs were fabricated in this way including all-organic, flexible structures with only one processing step needed for semiconductor and dielectric.

In summary, the use of vertically phase separated bilayers has several advantages for OFETs. Namely the reduction in number of processing steps required to make a device, the ability to easily make both top- and bottom-gate devices, the control and improvement of interface properties especially with regard to intimate semiconductor–dielectric contact, and the possibility to incorporate encapsulation of the active material into the same processing step thus increasing device stability.

### 4.2 OFET self-assembly

The patterning or localisation of organic semiconductor on a substrate is useful for integrated circuit or display circuitry applications. This can be achieved by printing techniques, however, it would be simpler if an organic solution could be applied to the whole substrate and only remain where it is required. The tendency for blends to phase separate on deposition and therefore their ability to self-assemble, offers a way to form circuits in a single step. Such patterning has been demonstrated using various poly(3-alkylthiophenes) blended with poly(styrene).<sup>73</sup> Self-assembled monolayers such as thiols on gold and trichlorosilanes on SiO<sub>2</sub> were used to modify the surface energy and control where each phase was deposited, however, no functional devices were fabricated in this case.

Salleo and Arias<sup>74</sup> demonstrated OFET arrays using a polymer blend by controlling substrate surface conditions and propensity of each phase to de-wet during phase separation. The material system employed was a blend of regioregular poly(3,3'-didodecyl quaterthiophene) (PQT-12) with PMMA. Patterned OTS treatment was then used to define the OFET locations by

introducing a hydrophobic region on the predominately hydrophilic substrate. During spin coating of the solution both lateral and vertical phase separation occurred leading to the PQT-12-rich phase preferentially forming on the OTS treated region and overall encapsulation of the devices with PMMA (Fig. 14). A surface-directed spinodal decomposition mechanism is proposed with an initial PQT-12 wetting layer forming before lateral segregation occurs. Excess PQT-12 remains in the PMMA matrix as small but non-interconnected islands. This system therefore not only produces an array of OFETs but also improves air stability due to the self-encapsulation.<sup>75</sup> Processing and drying of the film must occur relatively rapidly since such a film morphology is metastable. Thermal annealing improves the PQT-12 crystallinity and therefore device performance, however, allowing diffusion of material at the polymer-polymer interfaces by solvent annealing leads to a loss of vertical phase separation and a homogenous, bulk de-mixed morphology.

## 5. Conclusions and outlook

The technique of blending organic semiconductors for solution processing is now being commonly employed in organic electronics, and thin film transistors are no exception. This has been partly due to the ease with which two or more components can be deposited from solution, and partly the ability to combine a wide

range of useful properties and even the potential for synergistic effects. Examples of desirable OFET features include high charge carrier mobility, ambipolar conduction, air stability, device-to-device uniformity and material self-assembly. Finding single materials that can satisfy several of these requirements is not always easy. However, there are also challenges involved with the use of multi-component blends especially regarding the control of film morphology, phase separation and the location of each component within the film.

In this paper we have reviewed the progress of solution-processed OFETs fabricated using semiconductor blends. The number of functional blend systems has increased as an understanding of the links between electrical properties and blend morphology has developed. Examples include the percolation pathways for holes and electrons in ambipolar OFETs such as PCBM : polymer blends, the optimisation and use of vertical phase separation to position high mobility components within the channel region of devices, or the ability to control when crystallisation of the semiconductor occurs during processing such as in rubrene : diphenylanthracene hypereutectic blends. Within all of these systems an important factor is the understanding of phase separation at various stages during solution processing techniques that are often far from equilibrium, such as spin coating or printing. Simple composition or temperature changes can be used to control the final microstructure but in addition it is vital to be able to alter substrate surface properties, solvent evaporation rates and viscosities, and solute-solute or solute-solvent interactions. This is especially true if we wish to use these systems on an industrial scale where film uniformity and low device-to-device variation is needed in combination with high mobility and/or the ability to create complementary or complementary-like logic circuits. Furthermore an understanding of charge conduction mechanisms in blend devices and how the film microstructure correlates to OFET performance is needed in order to optimise the processing for a particular application. However, there is great potential to use multi-component systems in OFET and organic circuit fabrication. The ultimate aim being large area, high mobility systems that can self-assemble with minimal processing, and allow gate dielectric and n- and p-type semiconductor positioning with suitable morphologies or crystallographic orientations in the OFET channels.

## Acknowledgements

We are grateful to the Engineering and Physical Sciences Research Council (EPSRC) grant numbers EP/C539516, EP/E02730X and Research Councils UK (RCUK) for financial support.

## References

- 1 B. H. Hamadani, D. J. Gundlach, I. McCulloch and M. Heeney, *Appl. Phys. Lett.*, 2007, **91**, 243512.
- 2 S. K. Park, D. A. Mourey, S. Subramanian, J. E. Anthony and T. N. Jackson, *Appl. Phys. Lett.*, 2008, **93**, 043301; A. Facchetti, *Mater. Today*, 2007, **10**, 28.
- 3 S. R. Forrest, *Nature*, 2004, **428**, 911.
- 4 B. Crone, A. Dodabalapur, Y.-Y. Lin, R. W. Filas, Z. Bao, A. LaDuca, R. Sarpeshkar, H. E. Katz and W. Li, *Nature*, 2000, **403**, 521.

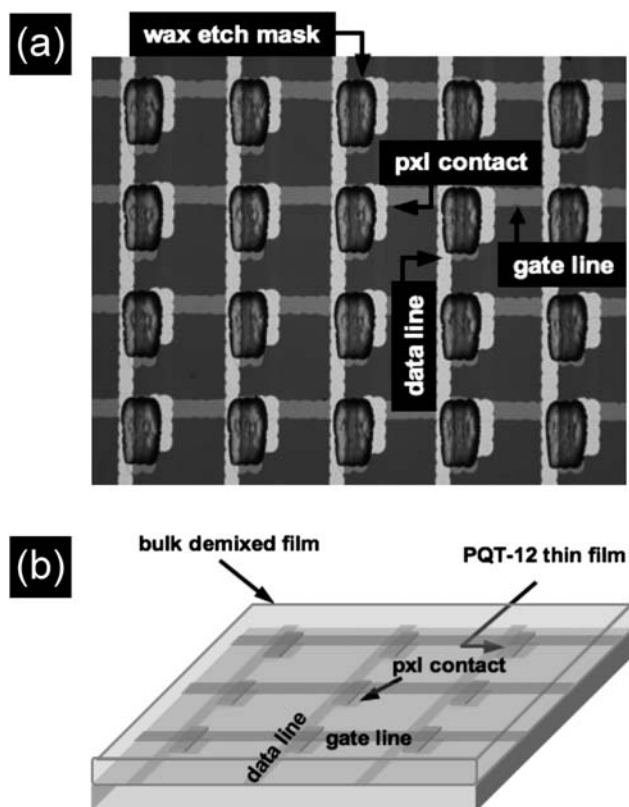


**Fig. 14** (a) The mask and substrate used to pattern OTS for a self-assembled OFET array using PQT-12 blended with PMMA. (b) Schematic of the thin film structure demonstrating the isolation of each PQT-12 transistor and the overall encapsulation of the array. Adopted from ref. 74 (Copyright Wiley-VCH Verlag GmbH & Co. KGaA. Reproduced with permission).



- 5 H. Hoppe and N. S. Sariciftci, *J. Mater. Chem.*, 2006, **16**, 45.
- 6 A. C. Arias, *J. Macromol. Sci. C: Polymer Reviews*, 2005, **46**, 103; E. Moons, *J. Phys.: Condens. Matter*, 2002, **14**, 12235.
- 7 M. Berggren, D. Nilsson and N. D. Robinson, *Nat. Mater.*, 2007, **6**, 3; S. P. Speakman, G. G. Rozenberg, K. J. Clay, W. I. Milne, A. Ille, I. A. Gardner, E. Bresler and J. H. G. Steinke, *Org. Electron.*, 2001, **2**, 65.
- 8 G. H. Gelinck, H. E. A. Huitema, E. v. Veenendaal, E. Cantatore, L. Schrijnemakers, J. B. P. H. v. d. Putten, T. C. T. Geuns, M. Beenhakkers, J. B. Giesbers, B.-H. Huisman, E. J. Meijer, E. M. Benito, F. J. Touwslager, A. W. Marsman, B. J. E. v. Rens and D. M. de Leeuw, *Nat. Mater.*, 2004, **3**, 106.
- 9 G. Horowitz, *J. Mater. Res.*, 2004, **19**, 1946.
- 10 C. Tanase, E. J. Meijer, P. W. M. Blom and D. M. de Leeuw, *Phys. Rev. Lett.*, 2003, **91**, 216601.
- 11 D. C. Coffey, O. G. Reid, D. B. Rodovsky, G. P. Bartholomew and D. S. Ginger, *Nano Lett.*, 2007, **7**, 738.
- 12 V. Podzorov, E. Menard, A. Borissov, V. Kiryukhin, J. A. Rogers and M. E. Gershenson, *Phys. Rev. Lett.*, 2004, **93**, 086602.
- 13 G. Horowitz and P. Delannoy, *J. Appl. Phys.*, 1991, **70**, 469.
- 14 L. M. Robeson, *Polymer Blends: A Comprehensive Review*, Hanser Verlag, 2007; P. J. Flory, *Principles of polymer chemistry*, Cornell University Press, 1953.
- 15 P. J. Flory, *J. Chem. Phys.*, 1942, **10**, 51.
- 16 J. W. Cahn and J. E. Hilliard, *J. Chem. Phys.*, 1958, **28**, 258.
- 17 N. P. Balsara, C. Lin and B. Hammouda, *Phys. Rev. Lett.*, 1996, **77**, 3847, LP.
- 18 R. A. L. Jones, L. J. Norton, E. J. Kramer, F. S. Bates and P. Wiltzius, *Phys. Rev. Lett.*, 1991, **66**, 1326.
- 19 C. M. Björström, S. Nilsson, A. Bernasik, A. Budkowski, M. Andersson, K. O. Magnusson and E. Moons, *Appl. Surf. Sci.*, 2007, **253**, 3906.
- 20 S. Y. Heriot and R. A. L. Jones, *Nat. Mater.*, 2005, **4**, 782.
- 21 J.-S. Kim, P. K. H. Ho, C. E. Murphy and R. H. Friend, *Macromolecules*, 2004, **37**, 2861.
- 22 C. M. Björström, K. O. Magnusson and E. Moons, *Synth. Met.*, 2005, **152**, 109.
- 23 C. Ton-That, A. G. Shard, D. O. H. Teare and R. H. Bradley, *Polymer*, 2001, **42**, 1121; A. M. Higgins, S. J. Martin, R. L. Thompson, J. Chappell, M. Voigt, D. G. Lidzey, R. A. L. Jones and M. Geoghegan, *J. Phys.: Condens. Matter*, 2005, **17**, 1319.
- 24 J. C. Wittmann and R. S. J. Manley, *J. Polym. Sci., Polym. Phys. Ed.*, 1977, **15**, 1089.
- 25 W. Zhang, J. Smith, R. Hamilton, M. Heeney, J. Kirkpatrick, K. Song, S. E. Watkins, T. Anthopoulos and I. McCulloch, *J. Am. Chem. Soc.*, 2009, **131**, 10814.
- 26 S. K. Park, T. N. Jackson, J. E. Anthony and D. A. Mourey, *Appl. Phys. Lett.*, 2007, **91**, 063514.
- 27 K. C. Dickey, J. E. Anthony and Y.-L. Loo, *Adv. Mater.*, 2006, **18**, 1721.
- 28 S. Liu, W. M. Wang, A. L. Briseno, S. C. B. Mannsfeld and Z. Bao, *Adv. Mater.*, 2009, **21**, 1217.
- 29 H. L. Wang and J. E. Fernandez, *Macromolecules*, 1993, **26**, 3336.
- 30 J. Zaumseil and H. Sirringhaus, *Chem. Rev.*, 2007, **107**, 1296.
- 31 A. Dodabalapur, J. Laquindanum, H. E. Katz and Z. Bao, *Appl. Phys. Lett.*, 1996, **69**, 4227.
- 32 E. J. Meijer, D. M. De Leeuw, S. Setayesh, E. Van Veenendaal, B.-H. Huisman, P. W. M. Blom, J. C. Hummelen, U. Scherf and T. M. Klapwijk, *Nat. Mater.*, 2003, **2**, 678.
- 33 T. D. Anthopoulos, S. Setayesh, E. Smits, M. Cölle, E. Cantatore, B. de Boer, P. W. M. Blom and D. M. de Leeuw, *Adv. Mater.*, 2006, **18**, 1900.
- 34 L.-L. Chua, J. Zaumseil, J.-F. Chang, E. C.-W. Ou, P. K.-H. Ho, H. Sirringhaus and R. H. Friend, *Nature*, 2005, **434**, 194.
- 35 D. M. de Leeuw, M. M. J. Simenon, A. R. Brown and R. E. F. Einerhand, *Synth. Met.*, 1997, **87**, 53; T. D. Anthopoulos, G. C. Anyfantis, G. C. Papavassiliou and D. M. de Leeuw, *Appl. Phys. Lett.*, 2007, **90**, 122105; K. Takimiya, T. Yamamoto, H. Ebata and T. Izawa, *Sci. Technol. Adv. Mater.*, 2007, **8**, 273.
- 36 W. Geens, S. E. Shaheen, C. J. Brabec, J. Poortmans and N. S. Sariciftci, in *Electronic Properties of Novel Materials - Molecular Nanostructures: XIV International Winterschool Euroconference*, ed. H. Kuzmany, J. Fink, M. Mehring and S. Roth, AIP, Kirchberg, Austria, 2000, pp. 516.
- 37 Y. Hayashi, H. Kanamori, I. Yamada, A. Takasu, S. Takagi and K. Kaneko, *Appl. Phys. Lett.*, 2005, **86**, 052104.
- 38 T. B. Singh, S. Günes, N. Marjanović, N. S. Sariciftci and R. Menon, *J. Appl. Phys.*, 2005, **97**, 114508.
- 39 E. von Hauff, J. Parisi and V. Dyakonov, *Thin Solid Films*, 2006, **511**–**512**, 506.
- 40 S. Cho, J. Yuen, J. Y. Kim, K. Lee and A. J. Heeger, *Appl. Phys. Lett.*, 2006, **89**, 153505.
- 41 M. Campoy-Quiles, T. Ferenczi, T. Agostinelli, P. G. Etchegoin, Y. Kim, T. D. Anthopoulos, P. N. Stavrinou, D. D. C. Bradley and J. Nelson, *Nat. Mater.*, 2008, **7**, 158; Z. Xu, L.-M. Chen, G. Yang, C.-H. Huang, J. Hou, Y. Wu, G. Li, C.-S. Hsu and Y. Yang, *Adv. Funct. Mater.*, 2009, **19**, 1227.
- 42 A. Babel, J. D. Wind and S. A. Jenekhe, *Adv. Funct. Mater.*, 2004, **14**, 891.
- 43 A. Babel and S. A. Jenekhe, *J. Phys. Chem. B*, 2002, **106**, 6129.
- 44 I. McCulloch, M. Heeney, C. Bailey, K. Genevicius, I. MacDonald, M. Shkunov, D. Sparrowe, S. Tierney, R. Wagner, W. Zhang, M. L. Chabinyc, R. J. Kline, M. D. McGehee and M. F. Toney, *Nat. Mater.*, 2006, **5**, 328.
- 45 Z. Bao, A. Dodabalapur and A. J. Lovinger, *Appl. Phys. Lett.*, 1996, **69**, 4108.
- 46 N. Stingelin-Stutzmann, E. Smits, H. Wondergem, C. Tanase, P. Blom, P. Smith and D. de Leeuw, *Nat. Mater.*, 2005, **4**, 601.
- 47 S. Goffri, C. Müller, N. Stingelin-Stutzmann, D. W. Breiby, C. P. Radano, J. W. Andreasen, R. Thompson, R. A. J. Janssen, M. M. Nielsen, P. Smith and H. Sirringhaus, *Nat. Mater.*, 2006, **5**, 950.
- 48 F. Garnier, A. Yassar, R. Hajlaoui, G. Horowitz, F. Deloffre, B. Servet, S. Ries and P. Alnot, *J. Am. Chem. Soc.*, 1993, **115**, 8716.
- 49 D. M. Russell, C. J. Newsome, S. P. Li, T. Kugler, M. Ishida and T. Shimoda, *Appl. Phys. Lett.*, 2005, **87**, 222109.
- 50 R. A. Street, J. E. Northrup and A. Salleo, *Phys. Rev. B: Condens. Matter Mater. Phys.*, 2005, **71**, 165202.
- 51 E. Lim, B.-J. Jung, M. Chikamatsu, R. Azumi, K. Yase, L.-M. Do and H.-K. Shim, *Org. Electron.*, 2008, **9**, 952.
- 52 P. Wolfer, C. Müller, P. Smith, M. A. Baklar and N. Stingelin-Stutzmann, *Synth. Met.*, 2007, **157**, 827.
- 53 G. Horowitz, R. Hajlaoui, D. Fichou and A. E. Kassmi, *J. Appl. Phys.*, 1999, **85**, 3202.
- 54 Y.-Y. Lin, D. J. Gundlach, S. F. Nelson and T. N. Jackson, *IEEE Electron Device Lett.*, 1997, **18**, 606; T. W. Kelley, P. F. Baude, C. Gerlach, D. E. Ender, D. Muires, M. A. Haase, D. E. Vogel and S. D. Theiss, *Chem. Mater.*, 2004, **16**, 4413.
- 55 T. Minakata and Y. Natsume, *Synth. Met.*, 2005, **153**, 1.
- 56 J. E. Anthony, J. S. Brooks, D. L. Eaton and S. R. Parkin, *J. Am. Chem. Soc.*, 2001, **123**, 9482; C. D. Sheraw, T. N. Jackson, D. L. Eaton and J. E. Anthony, *Adv. Mater.*, 2003, **15**, 2009.
- 57 S. Subramanian, S. K. Park, S. R. Parkin, V. Podzorov, T. N. Jackson and J. E. Anthony, *J. Am. Chem. Soc.*, 2008, **130**, 2706.
- 58 B. A. Brown, J. Veres, R. M. Anemian, R. T. Williams, S. D. Ogier and S. W. Leeming, WO/2005/055248, 2005.
- 59 R. Hamilton, J. Smith, S. Ogier, M. Heeney, J. E. Anthony, I. McCulloch, D. D. C. Bradley, J. Veres and T. D. Anthopoulos, *Adv. Mater.*, 2009, **21**, 1166.
- 60 A. Bernasik, J. Rysz, A. Budkowski, K. Kowalski, J. Camra and J. Jedlinaski, *Macromol. Rapid Commun.*, 2001, **22**, 829.
- 61 T. Ohe, M. Kuribayashi, R. Yasuda, A. Tsuboi, K. Nomoto, K. Satori, M. Itabashi and J. Kasahara, *Appl. Phys. Lett.*, 2008, **93**, 053303.
- 62 J. Smith, R. Hamilton, I. McCulloch, M. Heeney, J. E. Anthony, D. D. C. Bradley and T. D. Anthopoulos, *Synth. Met.*, 2009, **159**, 2365.
- 63 W. H. Lee, J. A. Lim, D. Kwak, J. H. Cho, H. S. Lee, H. H. Choi and K. Cho, *Adv. Mater.*, 2009, **21**, 4243.
- 64 J. Smith, R. Hamilton, M. Heeney, D. M. de Leeuw, E. Cantatore, J. E. Anthony, I. McCulloch, D. D. C. Bradley and T. D. Anthopoulos, *Appl. Phys. Lett.*, 2008, **93**, 253301.
- 65 J. Kang, N. Shin, D. Y. Jang, V. M. Prabhu and D. Y. Yoon, *J. Am. Chem. Soc.*, 2008, **130**, 12273.
- 66 M. M. Payne, S. R. Parkin, J. E. Anthony, C.-C. Kuo and T. N. Jackson, *J. Am. Chem. Soc.*, 2005, **127**, 4986.
- 67 J.-H. Kwon, S.-I. Shin, K.-H. Kim, M. J. Cho, K. N. Kim, D. H. Choi and B.-K. Ju, *Appl. Phys. Lett.*, 2009, **94**, 013506.

- 
- 68 M.-B. Madec, D. Crouch, G. R. Llorente, T. J. Whittle, M. Geoghegan and S. G. Yeates, *J. Mater. Chem.*, 2008, **18**, 3230.
- 69 L.-L. Chua, P. K. H. Ho, H. Sirringhaus and R. H. Friend, *Adv. Mater.*, 2004, **16**, 1609.
- 70 D. S. Chung, D. H. Lee, J. W. Park, J. Jang, S. Nam, Y.-H. Kim, S.-K. Kwon and C. E. Park, *Org. Electron.*, 2009, **10**, 1041.
- 71 J. Veres, S. Ogier, S. W. Leeming, D. C. Cupertino and S. M. Khaffaf, *Adv. Funct. Mater.*, 2003, **13**, 199.
- 72 L. Qiu, J. A. Lim, X. Wang, W. H. Lee, M. Hwang and K. Cho, *Adv. Mater.*, 2008, **20**, 1141.
- 73 J. Jaczewska, A. Budkowski, A. Bernasik, I. Raptis, E. Moons, D. Goustouridis, J. Haberko and J. Rysz, *Soft Matter*, 2009, **5**, 234.
- 74 A. Salleo and A. C. Arias, *Adv. Mater.*, 2007, **19**, 3540.
- 75 A. C. Arias, F. Endicott and R. A. Street, *Adv. Mater.*, 2006, **18**, 2900.